International Conference on Mathematics, Computational Methods & Reactor Physics (M&C 2009)
Saratoga Springs, New York, May 3-7, 2009, on CD-ROM, American Nuclear Society, LaGrange Park, IL (2009)

A TIME-DEPENDENT FLECK FACTOR TO ENHANCE THE ACCURACY OF THE IMPLICIT MONTE CARLO EQUATIONS

Allan B. Wollaber
Argonne National Laboratory
9700 S. Cass Ave. Argonne, IL 64039
awollaber@anl.gov

Edward W. Larsen
Department of Nuclear Engineering and Radiological Sciences
University of Michigan
2355 Bonisteel Blvd, Ann Arbor, Michigan 48109
edlarsen@umich.edu

ABSTRACT

In the derivation of the Fleck and Cummings Implicit Monte Carlo (IMC) equations, an approximation is made that equates the time-averaged values of two unknowns with their "instantaneous" values. We demonstrate how this approximation can be avoided, thereby improving the accuracy of the resulting IMC equations and eliminating the need for defining the numerical parameter α. This leads to IMC equations that contain a time-dependent Fleck factor $f_n(t)$ instead of the traditional constant Fleck factor f_n during the n^{th} time step. We refer to the resulting equations as the IMC-TDF equations (IMC equations with a time-dependent Fleck factor). These equations may be solved using a Monte Carlo procedure that is comparable to the standard IMC procedure except for "extra" calculations to account for the time-dependence in $f_n(t)$. For linear problems, the IMC-TDF equations are second-order accurate with regard to reductions of the time step size (as are the IMC equations with $\alpha = 0.5$, although in practice most users set $\alpha = 1$ for stability considerations). For larger time steps, the IMC-TDF method behaves more like IMC with $\alpha = 1$. Numerical results are presented for 1-D, nonlinear gray and frequency-dependent problems. These demonstrate that computational solutions of the IMC-TDF equations are comparable in expense for small or moderate time steps, but can be more expensive than the IMC equations for large time steps.

Key Words: Implicit Monte Carlo, radiative transfer

1. INTRODUCTION

The Implicit Monte Carlo (IMC) method due to Fleck and Cummings [1] has been regularly employed in thermal radiative transport (TRT) problems for approximately 30 years despite several well-known deficiencies [2–4] and the emergence of alternative methodologies [5]. However, with the exception of a very recent suggestion to adaptively modify the Fleck factor [6], the IMC formulation has remained largely unchanged. In this paper, we develop and implement a more accurate form of the IMC equations by reducing the approximation made in their derivation.

Arguably, the most dubious approximation that takes place in the derivation of the Fleck and Cummings Implicit Monte Carlo (IMC) equations occurs when the time-average unknowns for the "equilibrium" radiative energy density $\overline{U_r}$ and angular intensity $\overline{I}$ are replaced by their

"instantaneous" counterparts $U_r(t)$ and $I(t)$ [1]. The resulting expression for $U_r(t)$ is only correct in a time-average sense; in addition, it is not exact at the beginning of the time step $t = t_n$. In this paper, we replace this step by a different, more accurate approximation that preserves the character of the IMC equations at the expense of adding a new, *time-dependent* Fleck factor. We refer to this as the IMC-TDF approach (Implicit Monte Carlo with a Time-Dependent Fleck factor). This approach also avoids the introduction of the user-defined parameter α. We discuss the stability and implementation characteristics of these new equations as compared with the IMC equations. We suggest an "adaptive α" approach that could be used as a simple first step towards a full implementation of the IMC-TDF equations.* We present numerical test problems that demonstrate potential gains in accuracy from the IMC-TDF approach and comparable solution efficiencies to IMC for small to moderate time steps. For large time steps, we show that the IMC-TDF calculation can take much longer, and for this we suggest a simple modification to the time-dependent Fleck factor.

2. IMC EQUATIONS WITH A TIME-DEPENDENT FLECK FACTOR

For demonstration purposes, we begin from the 1-D, nonlinear, frequency-dependent thermal radiative transfer (TRT) equations with no scattering, although extension to 3-D is trivial. The radiation transport equation is:

$$\frac{1}{c}\frac{\partial I}{\partial t} + \mu\frac{\partial I}{\partial x} + \sigma_a I = \frac{1}{2}\sigma_a bcU_r + \frac{Q}{2}\,, \tag{1a}$$

with the energy balance equation:

$$\frac{1}{\beta}\frac{\partial U_r}{\partial t} + \sigma_p cU_r = \iint \sigma_a I \; d\mu' d\nu'\,, \tag{1b}$$

(equivalently):

$$\frac{\partial U_m}{\partial t} + \sigma_p cU_r = \iint \sigma_a I \; d\mu' d\nu'\,. \tag{1c}$$

In these equations, the unknowns are the specific intensity $I = I(x, \nu, \mu, t)$, the material energy density $U_m = U_m(x, t)$, and the "equilibrium" radiative energy density $U_r = U_r(x, t) = aT^4$. The material temperature T is related to the material energy density U_m by the specific heat c_v:

$$c_v = \frac{dU_m(T)}{dT}\,, \tag{2}$$

β is given by

$$\beta(x,t) = \frac{\partial U_r}{\partial U_m} = \frac{dU_r}{dT}\frac{dT}{dU_m}\,, \tag{3}$$

the normalized Planck spectrum b is

$$b = b(\nu, T) = \frac{15\nu^3}{\pi^4 T^4}\left(e^{\nu/T} - 1\right)^{-1}\,, \tag{4}$$

the absorption opacity σ_a is given by

$$\sigma_a(\nu, T) = \frac{\gamma(x)}{\nu^3}\left(1 - e^{-\nu/T}\right)\,, \tag{5}$$

*This approach also implies an adaptive Fleck factor that could be used as an alternative to or incorporated into the independently obtained, but loosely-related formulation suggested in [6]. Such an idea is outside the scope of this paper.

and the Plank opacity σ_p is the result of frequency-weighting $\sigma_a(\nu)$ against the Planck spectrum $b(\nu, T)$.

The first approximation in deriving the IMC or IMC-TDF equations is to "freeze" the opacities and β at the initial time t_n, which destroys the equivalency of Eqs. (1b) and (1c). This produces the system:

$$\frac{1}{c}\frac{\partial I}{\partial t} + \mu\frac{\partial I}{\partial x} + \sigma_{a,n} I = \frac{1}{2}\sigma_{a,n} bcU_r + \frac{Q}{2}\,, \tag{6a}$$

$$\frac{1}{\beta_n}\frac{\partial U_r}{\partial t} + \sigma_{p,n} cU_r = \iint \sigma_{a,n} I \; d\mu' d\nu'\,, \tag{6b}$$

$$\frac{\partial U_m}{\partial t} + \sigma_{p,n} cU_r = \iint \sigma_{a,n} I \; d\mu' d\nu'\,. \tag{6c}$$

Here, we depart from Fleck and Cumming's approach and solve Eq. (6b) for $U_r(t)$:

$$\frac{\partial}{\partial t} U_r(t) e^{\beta_n \sigma_{p,n} c(t-t_n)} = e^{\beta_n \sigma_{p,n} c(t-t_n)} \beta_n \iint \sigma_{a,n} I(t) \; d\mu' d\nu'\,,$$

$$U_r(t) e^{\beta_n \sigma_{p,n} c(t-t_n)} - U_{r,n} = \int_{t_n}^{t} e^{\beta_n \sigma_{p,n} c(t'-t_n)} \beta_n \iint \sigma_{a,n} I(t') \; d\mu' \, d\nu' \, dt'\,.$$

This expression contains no additional approximations.[†] Here we approximate the time integral by treating $I(t)$ "implicitly":

$$\begin{aligned} U_r(t) e^{\beta_n \sigma_{p,n} c(t-t_n)} &\approx U_{r,n} + \int_{t_n}^{t} e^{\beta_n \sigma_{p,n} c(t'-t_n)} \beta_n \iint \sigma_{a,n} I(t) \; d\mu' \, d\nu' \, dt'\,, \\ &= U_{r,n} + \frac{1}{\sigma_{p,n} c}\left(e^{\beta_n \sigma_{p,n} c(t'-t_n)} - 1\right) \iint \sigma_{a,n} I(t) \; d\mu' \, d\nu'\,. \end{aligned}$$

Solving for $U_r(t)$, we obtain:

$$U_r(t) = U_{r,n} e^{-\beta_n \sigma_{p,n} c(t-t_n)} + \frac{1}{\sigma_{p,n} c}\left(1 - e^{-\beta_n \sigma_{p,n} c(t'-t_n)}\right) \iint \sigma_{a,n} I(t) \; d\mu' \, d\nu'\,. \tag{7}$$

Next, we define a *time-dependent Fleck factor* $f_n(t)$ as:

$$\boxed{f_n(t) = e^{-\beta_n \sigma_{p,n} c(t-t_n)}\,,} \tag{8}$$

and we rewrite Eq. (7) using Eq. (8) as:

$$U_r(t) = U_{r,n} f_n(t) + \frac{1 - f_n(t)}{\sigma_{p,n} c} \iint \sigma_{a,n} I(t) \; d\mu' \, d\nu'\,. \tag{9}$$

Eq. (8) and its ramification in Eq. (9) constitute the essential new results in this paper. For instance, Eq. (9) is exact at $t = t_n$. By comparison, the constant Fleck factor and corresponding equation for $U_r(t)$ are given for the traditional IMC method in [1] as:

$$f_n = \frac{1}{1 + \alpha \Delta_{t,n} \beta_n c \sigma_{p,n}}\,, \tag{10a}$$

[†] This is actually the final form employed in the Carter-Forest method [5].

$$U_r(t) = f_n U_{r,n} + \frac{(1-f_n)}{c\sigma_{p,n}} \iint \sigma_{a,n} I(t)\, d\mu' d\nu' \,. \tag{10b}$$

Clearly, Eq. (10b) cannot be exact at $t = t_n$ unless the user-defined parameter α is zero. However, for numerical stability, α must satisfy $0.5 \leq \alpha \leq 1$, and $\alpha = 1$ is almost always chosen in practice. We note that Eq. (9) has the same form as Eq. (10b), but the Fleck factor in Eq. (9) is time-dependent, which implies that the Monte Carlo procedure for the IMC-TDF equations will be similar to that of the IMC equations. We continue by introducing Eq. (9) into Eqs. (6a) and (6c). Substitution into Eq. (6a) yields:

$$\frac{1}{c}\frac{\partial I}{\partial t} + \mu\frac{\partial I}{\partial x} + \sigma_{a,n} I = \frac{1}{2}\sigma_{a,n} bc \left(U_{r,n} f_n(t) + \frac{1-f_n(t)}{\sigma_{p,n} c} \iint \sigma_{a,n} I(t)\; d\mu'\, d\nu' \right) + \frac{Q}{2} \,. \tag{11}$$

Introducing the frequency spectrum $\chi_n(\nu)$

$$\chi_n = \chi_n(x,\nu) \equiv \frac{\sigma_{a,n} b_n}{\int \sigma_{a,n} b_n \; d\nu'} = \frac{\sigma_{a,n} b_n}{\sigma_{p,n}} = \frac{1}{T_n} e^{-\nu/T_n} \,, \tag{12}$$

into Eq. (11), we obtain the first of the IMC-TDF equations:

$$\frac{1}{c}\frac{\partial I}{\partial t} + \mu\frac{\partial I}{\partial x} + \sigma_{a,n} I = \frac{1}{2} f_n(t) \sigma_{a,n} b_n c U_{r,n} + \frac{1}{2}\chi_n \iint (1 - f_n(t)) \sigma_{a,n} I \; d\mu' d\nu' + \frac{Q}{2} \,. \tag{13}$$

Next we introduce the same approximations into Eq. (6c) to obtain the following equation for $U_{m,n+1}$:

$$\frac{\partial U_m}{\partial t} + f_n(t)\sigma_{p,n} c U_{r,n} = f_n(t) \iint \sigma_{a,n} I(t)\, d\mu' d\nu' \,. \tag{14}$$

Eq. (14) may then be integrated over the time step defined by $t_n \leq t \leq t_{n+1}$ with $\Delta_{t,n} = t_{n+1} - t_n$ to obtain the update equation for the material energy density (the second of the IMC-TDF equations):

$$U_{m,n+1} = U_{m,n} - \frac{U_{r,n}}{\beta_n}\left(1 - e^{-\sigma_{p,n}\beta_n c \Delta_{t,n}}\right) + \int_{t_n}^{t_{n+1}} \iint f_n(t)\sigma_{a,n} I(t)\, d\mu' d\nu' dt \,.$$

Once $U_{m,n+1}$ is calculated, the temperature T_{n+1} can be updated as usual by solving:

$$U_{m,n+1} = \int_0^{T_{n+1}} c_v(T')\; dT' \,. \tag{15}$$

In the case of a perfect gas, this reduces to $T_{n+1} = U_{m,n+1}/c_v$.

None of the approximations introduced here violates the conservation of energy. This may be verified by integrating Eq. (13) over frequency and angle and adding it to Eq. (14) to obtain the energy balance equation:

$$\frac{\partial}{\partial t}\left(\frac{1}{c}\iint I \; d\mu d\nu + U_m\right) = \int Q \; d\nu - \iint \mu\frac{\partial I}{\partial x} d\mu d\nu \,. \tag{16}$$

Eq. (16) is the same as that which may be obtained by manipulating the corresponding TRT equations [Eq. (1a) and Eq. (1c)].

To summarize, the IMC-TDF equations consist of the following radiation transport equation for I which is solved using a Monte Carlo process:

$$\frac{1}{c}\frac{\partial I}{\partial t} + \mu\frac{\partial I}{\partial x} + \sigma_{a,n}I = \frac{1}{2}f_n(t)\sigma_{a,n}b_n c U_{r,n} + \frac{\chi_n}{2}\iint (1 - f_n(t))\sigma_{a,n}I(t)\, d\mu' d\nu' + \frac{Q}{2}\,, \quad (17a)$$

and a material energy balance equation:

$$U_{m,n+1} = U_{m,n} - \frac{U_{r,n}}{\beta_n}\left(1 - e^{-\sigma_{p,n}\beta_n c\Delta_{t,n}}\right) + \int_{t_n}^{t_{n+1}}\iint f_n(t)\sigma_{a,n}I(t)\, d\mu' d\nu' dt\,, \quad (17b)$$

where $f_n(t)$ is defined in Eq. (8). The temperature T_{n+1} is calculated from:

$$U_{m,n+1} = \int_0^{T_{n+1}} c_v(T')\, dT'\,. \quad (17c)$$

2.1. Discussion

Eqs. (17) are analogous to the IMC equations except for the introduction of the time-dependent Fleck factor $f_n(t)$ defined in Eq. (8). We first consider how $f_n(t)$ compares to the usual f_n. To compare these two quantities directly, we employ a scaled time variable τ defined by $\tau = (\beta_n/4)\sigma_{p,n}t$. Then, we may more simply write the time-dependent terms as:

$$4(\tau - \tau_n) = \beta_n\sigma_{p,n}c(t - t_n)\,. \quad (18)$$

Here τ is the scaled time in mean free times for emission.[‡] Using Eq. (18) in Eq. (8), we write the scaled version of the time-dependent Fleck factor as

$$f_n(\tau) = e^{-4(\tau-\tau_n)}\,, \quad (19)$$

and the scaled version of the "traditional" Fleck factor in Eq. (10a) as:

$$f = \frac{1}{1 + 4\alpha\Delta_\tau}\,. \quad (20)$$

We also derive the average value of $f_n(\tau)$ over the time step, which we denote by $\overline{f_n(\tau)}$ (this is indirectly used to obtain the energy emitted by the material over the time step). This is:

$$\overline{f_n(\tau)} = \frac{1}{\Delta_\tau}\int_{\tau_n}^{\tau_{n+1}} f_n(\tau)\, d\tau = \frac{1}{4\Delta_\tau}\left(1 - e^{-4\Delta_\tau}\right)\,. \quad (21)$$

In Figure 1, we plot Eqs. (19), (20), and (21) over a unit, scaled time step. As expected, $f_n(\tau)$ begins at unity and exponentially decays, passing through each of the constant valued Fleck factors by the end of the time step. We first consider what the time-average effect of this behavior is.

In Figure 1, the averaged time-dependent Fleck factor falls between the traditional Fleck factors evaluated with $\alpha = 0.5$ and $\alpha = 1$. If $\Delta_\tau \approx 0$, we find that:

$$\overline{f_n(\tau)} = \frac{1}{4\Delta_\tau}\left[1 - (1 - 4\Delta_\tau + 8\Delta_\tau^2 + O(\Delta_\tau^3))\right]\,,$$

[‡]For a discussion about this scaling, see the companion paper on stability or [7].

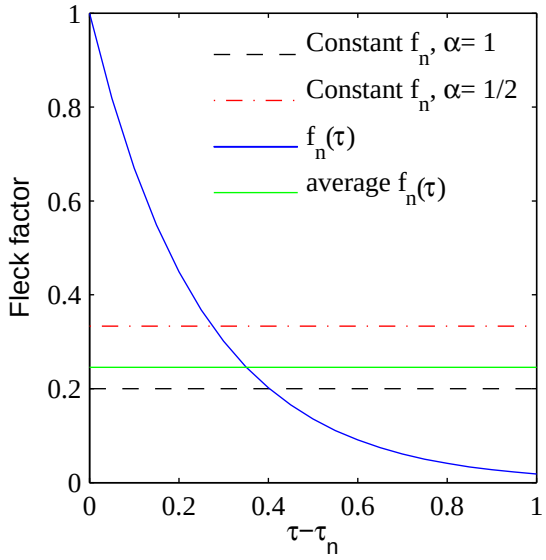

Figure 1. The Time-Dependent Fleck Factor Compared to the Traditional Fleck Factors During a Time Step.

$$\overline{f_n(\tau)} = 1 - 2\Delta_\tau + O(\Delta_\tau^2)\,. \tag{22a}$$

For the traditionally-defined constant Fleck factor, this limit is:

$$\frac{1}{1+4\alpha\Delta_\tau} = 1 - 4\alpha\Delta_\tau + O(\Delta_\tau^2)\,. \tag{22b}$$

Thus, in the limit of *small* time steps $\overline{f_n(\tau)}$ behaves, to first order, like the traditional Fleck factor with $\alpha = 1/2$. This is advantageous since it is known that using $\alpha = 1/2$ is the most accurate approach for small time steps [8].

For large time steps, the limiting values of the averaged time-dependent and constant Fleck factors are:

$$\overline{f_n(\tau)} = \frac{1}{4\Delta_\tau} + O\left(e^{-4\Delta_\tau}\right)\,, \tag{23a}$$

$$\frac{1}{1+4\alpha\Delta_\tau} = \frac{1}{4\alpha\Delta_\tau} + O\left(\frac{1}{\Delta_\tau^2}\right)\,, \tag{23b}$$

so that, in the limit of *large* time steps, the average $f_n(\tau)$ behaves, to first order, like the traditional Fleck factor with $\alpha = 1$. This is again advantageous since we know that for large time steps, using $\alpha = 1$ in the traditional IMC approach is the "safest" choice (it minimizes the damped temporal oscillations that would otherwise occur from using $\alpha < 1$).

Together, Figure 1 and the limiting conditions in Eqs. (22) and (23) suggest an alternative to using the IMC-TDF equations that could be used as a simple first step towards an true implementation of the IMC-TDF equations. Instead of using $f_n(\tau)$, its time average $\overline{f_n(\tau)}$ could

be employed to select an adaptive value of α for the IMC equations. Setting the traditional IMC Fleck factor in Eq. (20) to equal $\overline{f_n(\tau)}$ in Eq. (21) produces the following equation for α_{adapt}:

$$\alpha_{\text{adapt}} = \frac{1}{1 - e^{-4\Delta_\tau}} - \frac{1}{4\Delta_\tau}\,, \tag{24}$$

where, by the above asymptotic limits, $0.5 < \alpha_{\text{adapt}} < 1$. In unscaled variables, this is:

$$\alpha_{\text{adapt}} = \frac{1}{1 - e^{-\beta_n \sigma_{p,n} c \Delta_t}} - \frac{1}{\beta_n \sigma_{p,n} c \Delta_t}\,. \tag{25}$$

We note that this approach would not be as accurate as using the time-dependent Fleck factor, but it would be trivial to implement, and it should be investigated as future work. A loosely-related technique that incorporates an adaptive Fleck factor has recently been attempted with some success by McClarren [6], although it appears that McClarren's approach is mostly concerned with large time steps.

Because $\overline{f_n(\tau)}$ is larger than the traditional Fleck factor with $\alpha = 1$, the source term involving $U_{r,n}$ in Eq. (17a) will emit more energy during a time step than the corresponding IMC source term. By contrast, if $\alpha = 1/2$ is used in a regular IMC calculation, the source term in Eq. (17a) will be smaller.

Because the time-average of the time-dependent Fleck factor limits to the traditional Fleck factor with $\alpha = 1$ for large time steps, we conjecture that solutions of Eqs. (17) should also violate the maximum principle if sufficiently large time steps are used [2]. It is unclear if the same limit on the time step found in [2] is applicable to Eqs. (17). Later, we numerically verify that the IMC-TDF equations can violate the maximum principle. For the same reasons, we also conjecture that the IMC-TDF equations will likely not contain the equilibrium diffusion limit [3]. Thus, we expect the accuracy gains achievable by using the IMC-TDF method will primarily occur for short to moderately-sized time steps; IMC-TDF does little to ameliorate problems that occur for large time steps.

We next consider the time-dependent behavior of $f_n(\tau)$ shown in Figure 1. Recalling that the Fleck factor is the probability of an effective absorption, the exponential decay in $f_n(\tau)$ means that the overall probability of effective absorptions is *much* higher at the beginning of the time step than at the end. Particles born early in the time step are therefore much more likely to become absorbed into the material. On the other hand, $f_n(\tau)$ also appears on the right side of Eq. (17a) in the radiation source term that includes $U_{r,n}$. This implies that particle emission times due to this term are weighted to occur near the beginning of the time step. By contrast, the corresponding term in the traditional IMC equations is time-independent, and the corresponding particle emission times are uniform over the time step. One may argue directly from Eq. (7) that using an exponential distribution of the source particles due to the estimate of $U_r(t)$ should be more accurate than a time-independent source; using a time-independent source will overestimate the contribution of this term late in the time step. The overall effect of using $f_n(t)$ is that (i) Monte Carlo particles are much more likely to be born from the $U_{r,n}$ term near the beginning of the time step and (ii) these Monte Carlo particles are also more likely to undergo effective absorptions near the beginning of the time step, and effective scatters near the end. For large time steps, the dominance of the effective scattering can lead to a radiation equation that is highly

diffusive for the end of the time step. Under these conditions, it would likely be advantageous to incorporate one of the diffusive modifications to reduce the computational cost discussed in [9] or [10], although we do not consider that here.

We have performed a stability analysis of the IMC-TDF equations and found them to be unconditionally stable for a representative class of nonlinear problems. The IMC-TDF equations were also found to have monotonicity conditions that are slightly more restrictive than the IMC equations [7]. As an interesting aside, a seemingly benign counterpart to the time-dependent Fleck factor can be derived or expanded from Eq. (8) in the following rational form:

$$f_{\text{rat.,n}}(t) = \frac{1}{1 + \sigma_{p,n}\beta_n c(t - t_n)} \,. \tag{26}$$

Using this form of the time-dependent Fleck factor avoids the evaluation of "extra" exponential and logarithmic functions and should arguably be more accurate than IMC. However, using the same stability analysis, we found this approach to be conditionally stable with regard to the time step size, making this approach inadvisable. For details of this analysis, the reader is referred to [7] and to a companion paper on stability in these proceedings.

3. MONTE CARLO IMPLEMENTATION DIFFERENCES

Since $\overline{f_n(t)}$ differs from the traditionally defined f_n, the magnitude of the source energy due to the term containing $U_{r,n}$ also differs between the IMC-TDF and IMC equations. The new source energy is given by:

$$\begin{aligned} E_R &= \int_{t_n}^{t_{n+1}} \int_0^X \int_0^\infty \int_{-1}^1 \frac{1}{2}\chi_n(\nu) c f_n(t) \sigma_{p,n}(x) U_{r,n}(x) \, d\mu \, d\nu \, dx \, dt \,, \\ &= \frac{1}{\beta_n}\left(1 - e^{\beta_n \sigma_{p,n} c \Delta_{t,n}}\right) \int_0^X U_{r,n}(x) \, dx \,. \end{aligned} \tag{27}$$

This result is greater than that of the IMC equations when $\alpha = 1$ and lesser when $\alpha = 0.5$.

Next, the emission time due to this source is no longer uniform. Instead, the pdf for the emission time is:

$$p(t) = \beta_n \sigma_{p,n} c \frac{e^{-\beta_n \sigma_{p,n} c (t - t_n)}}{1 - e^{-\beta_n \sigma_{p,n} c \Delta_{t,n}}} \,. \tag{28}$$

To sample from this pdf using a Uniform Random Variate ξ, we use:

$$t = t_n - \frac{1}{\beta_n \sigma_{p,n} c} \ln\left[1 - \xi\left(1 - e^{-\beta_n \sigma_{p,n} c \Delta_{t,n}}\right)\right] \,. \tag{29}$$

Eq. (29) is the emission time of an IMC particle due to energy from E_R in Eq. (27). Using Eq. (29) will slightly increase the cost of the computation relative to the traditional IMC method, as the traditional IMC method does not require the evaluation of a logarithm for this term.

Finally, the probability of an effective absorption becomes time-dependent. Instead of storing f_n at the beginning of the time step, it is necessary to evaluate the exponential in Eq. (8) upon

each collision. This will also increase the computational cost of the calculation. These three changes are all that is required to convert an existing IMC code to one that employs a time-dependent Fleck factor, with one caveat concerning variance reduction in particle tracking. A reviewer noted that current IMC codes employ a continuous energy deposition technique for variance reduction (see [1]). In that case, it is necessary to either revert to collision-based tracking or to form a new probability density function (pdf) to sample a scattering collision location. This pdf can be formed by solving the following "scattering removal" equation for photons $N_{\mathrm{s.r.}}(s)$ along a flight path described over $0 < s < \infty$:

$$\frac{dN_{\mathrm{s.r.}}}{ds}(s) = -\left[1 - f_n(t(s))\right] \sigma_{a,n} N_{\mathrm{s.r.}}(s)\,, \tag{30}$$

which is of the form

$$\frac{dN_{\mathrm{s.r.}}}{ds} = -(1 - ae^{-bs})\sigma_n N_{\mathrm{s.r.}}(s)\,, \tag{31}$$

where the constants a, b are:

$$a = e^{\beta_n \sigma_{p,n} c t_n}\,, \tag{32}$$

$$b = \beta_n \sigma_{p,n}\,. \tag{33}$$

This system has solution

$$N_{\mathrm{s.r.}}(s) = C \exp\left(-\sigma_n \left(s - \frac{a}{b}\left(1 - e^{-bs}\right)\right)\right)\,, \tag{34}$$

where C is a normalization constant. Eq. (34) would be the unnormalized pdf to sample if continuous energy deposition is desired in the IMC-TDF equations. The usual technique of analytically inverting the cumulative density function for Eq. (34) may not be possible, although this pdf is predictable enough that an efficient rejection technique could be employed. Once a scattering collision distance s_c is found, it would then be necessary to determine the continuous energy deposition along the particle track. This is found by solving the related "absorption removal" problem for $N_{\mathrm{a.r.}}(s)$:

$$\frac{dN_{\mathrm{a.r.}}}{ds}(s) = -f_n(t(s))\sigma_{a,n} N_{\mathrm{a.r.}}(s)\,, \tag{35}$$

to find

$$N_{\mathrm{a.r.}}(s) = \exp\left(-\sigma_{a,n}\frac{a}{b}\left(1 - e^{-bs}\right)\right)\,, \tag{36}$$

The absorption energy deposited over the track length to collision location s_c would then be proportional to

$$\int_0^{s_c} N_{\mathrm{a.r.}}(s)ds = \int_0^{s_c} \exp\left(-\sigma_{a,n}\frac{a}{b}\left(1 - e^{-bs}\right)\right)\, ds\,, \tag{37}$$

This requires the evaluation of an exponential integral function $\mathrm{Ei}(s_c)$, but is otherwise analytically obtainable. We did not take this approach, opting instead for a simpler "implicit capture" technique.

4. NUMERICAL RESULTS

In this section we present numerical results for a 0-D linear problem, a 1-D, nonlinear gray Marshak wave problem, and a 1-D nonlinear frequency-dependent Marshak wave problem in order to characterize the accuracy and efficiency of IMC-TDF calculation.

4.1. Temporal Accuracy

To numerically assess the temporal order of accuracy, we consider a dimensionless, linear, gray, 0-D sample problem with $\sigma = a = c = 1$ and $c_v = 7.14T^3$. The temperature is set to an initial condition of 0.1, and the initial intensity ϕ is ≈ 2.79 (it is chosen to ensure that the equilibrium temperature is 1). The problem is solved using a variable number of time steps with an ending time fixed at $t = 10$, at which point the fine-mesh temperature solution is 1.0. To obtain numerical solutions of the IMC and IMC-TDF equations, we calculated exact numerical solutions of the IMC equations in [1] and Eqs. (17) applied to this linear, 0-D problem; no Monte Carlo calculation was performed. We define the root mean square error of the time-dependent temperature solutions by:

$$\text{RMS error} = \sqrt{\frac{1}{N}\sum_{n=1}^{N}\left(T_n - T_{\text{exact},n}\right)^2}, \tag{38}$$

where T_n is provided by an IMC method, and $T_{\text{exact},n}$ is the exact solution.

In Figure 2, we plot the RMS error of IMC methods that use $\alpha = 1$, $\alpha = 0.5$, and $f_n(t)$ defined in Eq. (8). The figure clearly shows the accuracy advantage of using the IMC-TDF equations; they are $O(\Delta_t^2)$ (at least for linear problems or, by extension, problem regions that are near equilibrium). Thus, the IMC-TDF equations retain the second-order accuracy in the time step for linear problems without the necessity of manually changing α from its usually-employed value to a less conservative value. We also observe that the IMC equations with $\alpha = 0.5$ are $O(\Delta_t^2)$, as has been previously demonstrated numerically in [8] for a slightly more difficult problem. However, $\alpha = 0.5$ is rarely used in practice, since it can lead to difficulties regarding damped, temporal oscillations. We remark that time steps as small as in the left side of Figure 2 are too short to be used in practice, but the intent of this figure is only to illustrate the asymptotic time convergence for a linear problem. We also remark that the Carter-Forest method is *exact* for this problem, although IMC remains the most widely used method.

4.2. Gray Marshak Wave Problems

In Wollaber's Ph.D. thesis [7], a numerically difficult nonlinear, gray Marshak wave problem is prescribed, analyzed, and solved using different approaches. This problem is described by using dimensionless variables obtained by setting $a = c = 1$, $c_v = 7.14$, $\sigma = T^{-3}$, and introducing the scaled time variable $\tau = (ac/c_v)t$.[§] The initial temperature is 0.1. We impose an isotropic right boundary condition equal to the initial temperature and an isotropic left boundary condition at 1.0. We consider a slab that is 4 cm wide. This implies that the slab is initially 4,000 mean free paths thick, but only 4 mean free paths thick once equilibrium is reached. We track the

[§]For more background on this scaling, we refer the reader to a companion paper on stability or to [7].

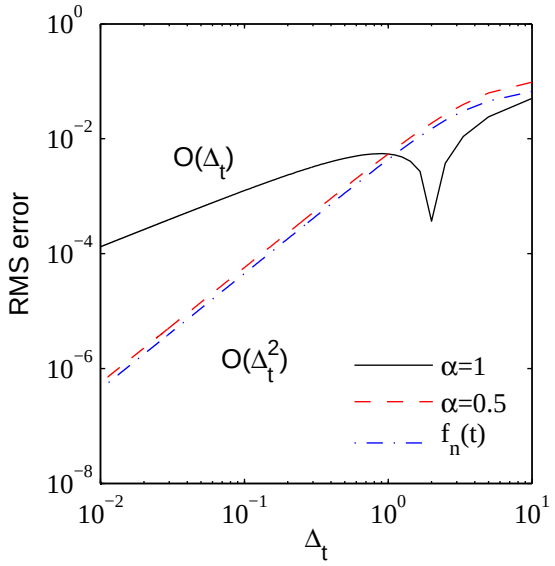

Figure 2. The Numerically-Calculated Order of Temporal Error for a Linear Problem for Traditional IMC with $\alpha = 1$ and $\alpha = 0.5$ and for IMC With the Time-Dependent Fleck Factor $f_n(t)$.

wavefront up to $\Delta_\tau = \Delta_t / c_v = 40$. The spatial grid and time step sizes are varied, and each problem is solved using a (self-written) Monte Carlo code.

The IMC solutions at the fixed time $\tau = 8$ are presented for variable cell sizes in Figure 3(a) and variable time step durations in Figure 3(b). In each of these figures we can see the worsening violations of the maximum principle [2] that result from increasing Δ_τ or decreasing Δ_x. Note that, because these figures are all depict temperature solutions at the *same* solution time, the "flattest" and right-most wave profile in each figure is the most accurate – ideally all the wave profiles should match this. The corresponding IMC-TDF wavefronts are provided as Figures 3(c) and 3(d) below their corresponding IMC solutions for ease of comparison. In the IMC-TDF solutions we observe that the degree of the maximum principle violation is slightly reduced for the larger time step sizes in Figure 3(c), but that the IMC-TDF solutions are just as sensitive as the IMC solutions with regard to reductions in the spatial cell size (Figure 3(d)). Unfortunately, the IMC-TDF method, although designed and shown to be more accurate than IMC with $\alpha = 1$ for smaller time steps, does not substantially outperform IMC for problems such as the violation of the maximum principle which emerge due to "long" time steps.

In a companion paper at this conference and in Wollaber's thesis [7], a new hybrid deterministic Monte Carlo method is introduced that enables the calculation of an appropriate time-averaged interpolated temperature T_* at which the temperature dependent quantities (i.e., σ, β, $B(\nu, T)$) in the IMC or IMC-TDF solutions may be evaluated. We refer to the IMC method with data evaluated at temperature T_* (instead of T_n) as the "IMC-T_*" method. Similarly, the IMC-TDF method with data evaluated at T_* is denoted as the "IMC-TDF-T_*" method. Using a more accurate temperature to evaluate the problem data in addition to the more accurate,

time-dependent Fleck factor is compelling, as these are the two primary sources of error (linearization and truncation) in the traditional formulation of the IMC equations. The IMC-TDF-T_* temperature solutions are also provided below the IMC and IMC-TDF solutions in Figure 3 as Figures 3(e) and 3(f). The suppression of the maximum principle violation that is obtained from using this approach easily surpasses either the IMC-TDF or the IMC-T_* methodologies alone.

With regard to solution efficiency, for the shortest time step employed ($\Delta_\tau = 0.1$), the IMC and IMC-TDF methods were within a few percent of each other in total computational time. For the longest time step used ($\Delta_\tau = 2$), the IMC-TDF solution took a maximum of 23% longer than the IMC solution. We noted above that the IMC-TDF calculation is expected to be more expensive than an IMC calculation; these results indicate that if short to reasonably-sized time steps are employed, the differences are minor. However, if "long" time steps are used, than the differences can become more severe, and the potential accuracy benefit is also diminished. This issue will be returned to below.

4.3. Frequency-Dependent Marshak Wave Problems

We next consider a frequency-dependent Marshak wave problem, primarily for the purposes of comparing solution efficiencies on a "realistic" problem. For this problem, $c \approx 300$ cm/sh and $a = 0.01372$ jk/cm^3-keV^4. The initial condition is an equilibrium state with a Planckian frequency distribution at $T = 0.01$ keV. At $t = 0$, the left side of the slab is subjected to an isotropic burst of radiation at a Planckian temperature $T = 1$ keV. The right boundary temperature is set to the constant, initial temperature. The slab size is 4 cm thick. The opacity coefficient [γ in Eq. (5)] is set to 200. The Planck mean opacity is therefore $30.8T^{-3}$ which means, at equilibrium ($T = 1$ keV), the slab is 123.2 Planck mean free paths thick, whereas at the initial condition $T = 0.01$, it is 123.2 $\times 10^6$ Planck mean free paths thick. The specific heat is set to 0.1 jk/keV-cc. We consider temperature solutions up to 1 sh. The spatial grid size Δ_x is set to 0.2 cm.

Each method used 100,000 particles/jk. To estimate relative errors and calculate figures of merit, each problem was independently simulated 50 times; the relative errors were then calculated using the sample error. All timing results refer to the sums of the computational times (not wall-clock times) reported by each processor. With the exception of "implicit capture", no variance reduction technique is employed in these calculations.

For the first case, we set Δ_t to 0.001 sh. Figure 4 depicts the IMC (solid) and IMC-TDF (dashed) temperature solutions at times of 0.3, 0.6, and 0.9 sh. For this choice of spatial and temporal grids, no difficulty emerges with regard to the maximum principle; the temperature wave forms and travels rightward (however, a reviewer noted that the spatial grid sizes employed here are much larger than is used in practice). With the possible exception of the leading edge of the wavefront, the solutions of the IMC and IMC-TDF methods agree well. We *conjecture* that the IMC wavefront is slightly more advanced (and less accurate) than the IMC-TDF wavefront because of the uniform probability of absorption for a given time step during the traversal of each spatial zone in the IMC approach. By comparison, absorption events in the IMC-TDF method are more likely at the beginning of a time step and (by extension) at the leading edges of each spatial zone. However, time and resource constraints have prevented a more thorough study of this behavior; so we turn to efficiency matters.

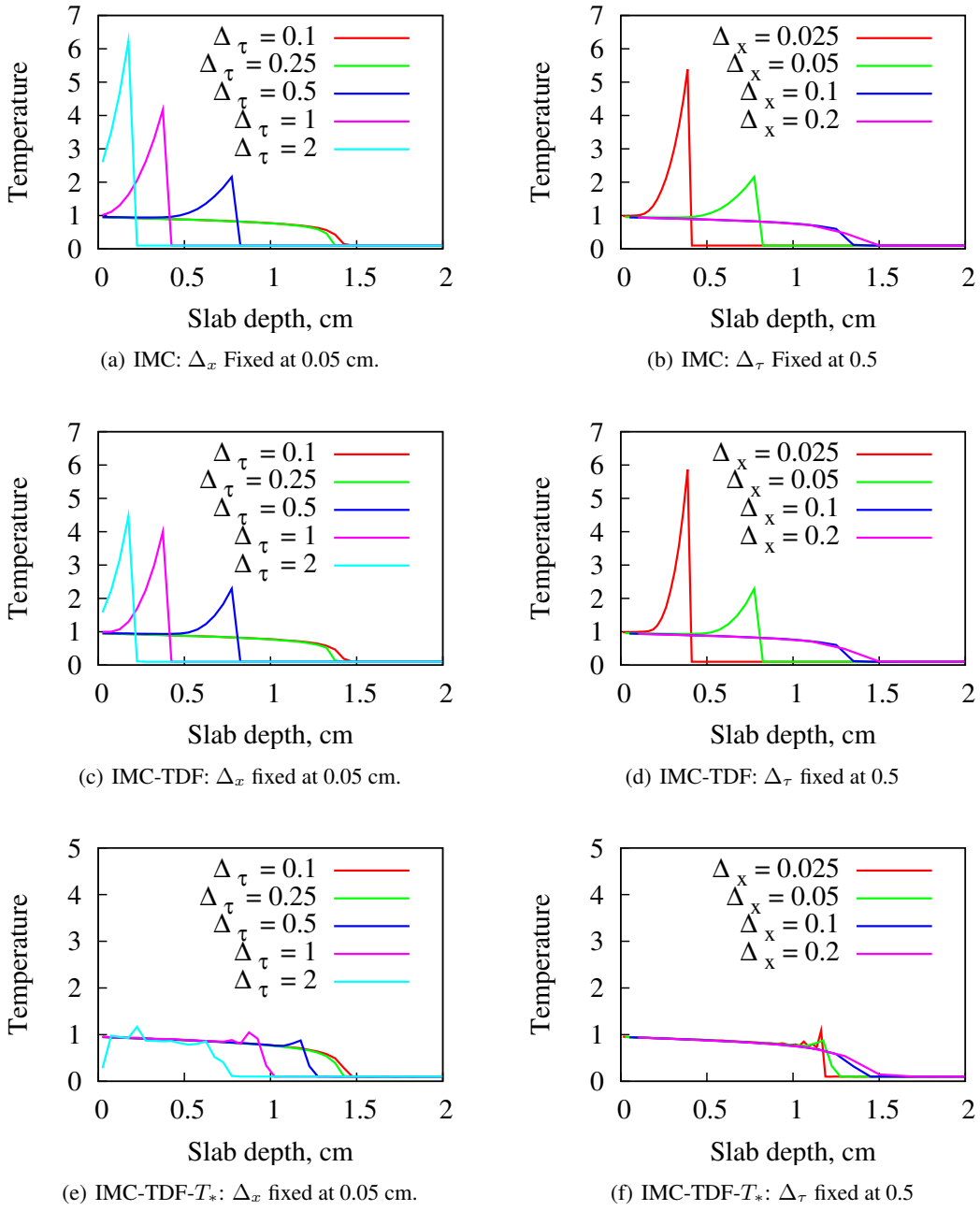

(a) IMC: Δ_x Fixed at 0.05 cm.

(b) IMC: Δ_τ Fixed at 0.5

(c) IMC-TDF: Δ_x fixed at 0.05 cm.

(d) IMC-TDF: Δ_τ fixed at 0.5

(e) IMC-TDF-T_*: Δ_x fixed at 0.05 cm.

(f) IMC-TDF-T_*: Δ_τ fixed at 0.5

Figure 3. Temperature Profiles at $\tau = 8$ for a Marshak Wave Problem in which [(a), (c), (e)] the Time Step is Varied and [(b), (d), (f)] the Spatial Grid Size is Varied Using "Traditional" IMC (Above), IMC-TDF (Middle), and IMC-TDF-T_* (Below).

The total time required for the IMC calculation is 74.4 CPU-hours. The total time required for the IMC-TDF simulation is 12.8 % less at 64.9 CPU-hours. It is not immediately obvious why the IMC-TDF method requires less calculation time for this problem, although it is heartening. However, when Δ_t is increased by a factor of 20 to 0.02 sh (a large time step size for this

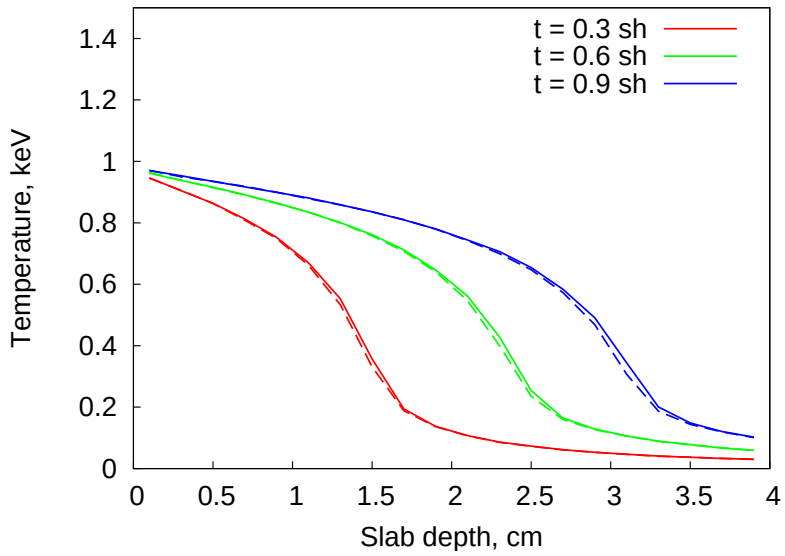

Figure 4. Temperature Profiles for a Frequency-Dependent Marshak Wave Problem Solved Using the IMC (Solid) and IMC-TDF (Dashed) Methods.

problem), the effect of this change on the CPU-time comparison is dramatic. The total time required by the IMC method is 59.4 hours, whereas the IMC-TDF method required 501.6 hours, an increase by a factor of 8.4. Upon inspection, nearly all of the CPU time disparity was found to occur during the first time step, during which the entire material is cold and thick and the IMC-TDF particles are forced to undergo a large number of effective scatter events.

The timing results of these two problems should not be solely relied upon as the final judgment of the IMC-TDF method; our intention is to demonstrate that for "reasonably-sized" time steps the methods are comparable in efficiency, but for large time steps the IMC-TDF calculation time can take much longer. It is unclear to what extent this behavior depends on the particularities of our implementation and this particular problem description. It is possible that using the continuous energy deposition approach for tracking and/or a lower weight cutoff mechanism (such as Russian roulette or a switch to analog tracking) could substantially reduce the differences. Additionally, a simple modification to $f_n(t)$ in Eq. (8) might also remedy this issue, as we next discuss.

4.4. Efficiency Degradation For Large Δ_t

We have shown that the solution times for the IMC and IMC-TDF methods compare well so long as the time step does not become too large. When the time step does become large, the IMC-TDF method can take much longer to simulate than the IMC method. This increase in cost is not balanced by a corresponding increase in accuracy, as both the IMC and IMC-TDF equations become inaccurate for large time steps.

As future work, it may be possible to remedy this problem by using a modified

time-dependent Fleck factor in which the effective scattering ratio is limited to the value used in the IMC equations with $\alpha = 1$. To illustrate this we use the dimensionless time variable $\tau = \sigma_{p,n}\beta_n ct$. We propose the following modification to $f_n(\tau)$:

$$f_n'(\tau) = \begin{cases} e^{-4(\tau-\tau_n)} & \tau_n \le \tau \le \tau_* \\ \frac{1}{1+4\Delta_\tau} & \tau_* < \tau \le \tau_{n+1} \end{cases}, \quad \tau_* = \tau_n + 0.5\ln(1+4\Delta_\tau)\,. \tag{39}$$

Thus, for $\tau \le \tau_*$, the time-dependent Fleck factor in Eq. (19) is used; for $\tau_* < \tau$, the "traditional", constant Fleck factor in Eq. (20) is used, and τ_* is chosen such that the two Fleck factors are equal. If the Fleck factor defined by Eq. (39) is used instead of Eq. (19), then the effective scattering ratio is limited by the traditional value used in Eq. (20). This modified time-dependent Fleck factor is designed to increase the accuracy of the IMC equations without significant increases in the required computational time. The implementation changes for the modified IMC-TDF equations would be slightly more complicated than the IMC-TDF equations, but not overly burdensome. For instance, the time-distribution of the source particles due to the $U_{r,n}$ term would no longer be purely exponential; it would be exponential for $\tau \le \tau_*$ and uniform for $\tau_* \le \tau$. Although we are unable to investigate this modified IMC-TDF method, we anticipate that it should retain the increase in accuracy for small time steps without corresponding increases in computational cost for large time steps.

5. CONCLUSIONS

In this paper we have presented an alternative, more accurate derivation of the IMC equations that leads to equations containing a time-dependent Fleck factor $f_n(t)$ [defined in Eq. (8)]: the IMC-TDF equations. Our derivation avoids the dubious approximation that occurs in [1] when time-average unknowns are replaced by "instantaneous" unknowns, and it eliminates the user-defined parameter α. The IMC-TDF equations retain the form of the IMC equations, so relatively few changes are necessary to modify existing computational algorithms for the IMC equations.

We discussed the properties of $f_n(t)$ and its time average to better elucidate their relationship to the usual Fleck factor. We suggested an "adaptive α" approach [see Eq. (24)] that could be used as a simple first step towards a full implementation of the IMC-TDF equations, and discussed how this adaptive α varies from 0.5 for short time steps to 1.0 for long steps. We discussed and numerically demonstrated how this property leads to $O(\Delta_t^2)$ temporal convergence for linear problems (i.e., problems with special material properties or that are near equilibrium).

We discussed how the IMC-TDF equations are unconditionally stable, although they have a slightly more restrictive monotonicity condition [7]. However, the IMC-TDF equations also share the deficiencies of IMC for long time steps, including the violation of the maximum principle [2] and (most likely) an inaccurate equilibrium diffusion limit [3]. This implies that the primary accuracy gains achievable by using the IMC-TDF formulation are for short to moderately-sized time steps; the IMC-TDF equations do little to address the problems that IMC solutions undergo for large time steps. It is possible that a combination of the IMC-TDF formulation and the approach suggested by McClarren [6] could improve the overall accuracy for the entire range of time step sizes.

We showed that for a series of nonlinear, Gray Marshak wave problems, the IMC-TDF solutions may still violate the maximum principle, but to a slightly lesser extent than the corresponding IMC solutions. However, when the IMC-TDF approach is combined with the IMC-T_* approach (in which the temperature-dependent quantities are evaluated at an appropriate time-averaged temperatures; see [7] or the companion paper in these proceedings), the suppression of the maximum principle violation is noteworthy. This is because the IMC-TDF equations suppress the time-discretization error, while the improved temperature evaluation suppresses the linearization error. For these problems, the IMC and IMC-TDF solution times were found to be comparable except for the largest time steps employed, which led to as much as a 23% increase.

We numerically tested the IMC-TDF procedure using a more realistic, nonlinear, frequency-dependent Marshak wave problem. For this problem, when a time step of $\Delta_t = 0.001$ sh was employed, the IMC and IMC-TDF solutions and computational times were found to be comparable, with IMC-TDF finishing about 12% faster. However, for the relatively large time step $\Delta_t = 0.02$ sh, the IMC-TDF calculation took over 8 times longer than IMC. It is unclear to what extent this behavior depends on the particularities of our implementation and our chosen problem description; more investigation is necessary to account for these discrepancies.

In conclusion, this paper describes a relatively simple enhancement to the accuracy of the IMC equations, especially for shorter to moderately sized time steps, and serves as a proof-of-principle for the idea. For future work, we have recommended a modification to $f_n(t)$ [see Eq. (39)] that may remedy the large discrepancies in runtimes for large time steps. We have also suggested an adaptive value to be used a simple first step towards integration into an IMC code [see Eq. (24)]. The effects of alternative Monte Carlo implementations such as continuous energy deposition in particle tracking [see Eq. (34)] should be investigated, and the IMC-TDF formulation should also be applied to a broader range of multidimensional test problems.

ACKNOWLEDGMENTS

This research was performed under appointment by the Department of Energy Computational Science Graduate Fellowship, which is provided under grant number DE-FG02-97ER25308.

REFERENCES

[1] J. A. Fleck, J. D. Cummings, "An Implicit Monte Carlo Scheme for Calculating Time and Frequency Dependent Nonlinear Radiation Transport," *J. of Comput. Phys.*, **8**, pp. 313–342 (1971).

[2] E. W. Larsen, B. Mercier, "Analysis of a Monte Carlo Method for Nonlinear Radiative Transfer," *J. Comput. Phys.*, **71**, pp. 50–64 (1987).

[3] J. D. Densmore, E. W. Larsen, "Asymptotic Equilibrium Diffusion Analysis of Time-Dependent Monte Carlo Methods for Grey Radiative Transfer," *J. Comput. Phys.*, **199**, pp. 175–204 (2004).

[4] N. Gentile, "A Comparison of Various Temporal Discretization Schemes for Infinite Media Radiation Transport," *Trans. Am. Nucl. Soc.*, **97**, pp. 544–546 (2007).

[5] W. R. Martin, F. B. Brown, "Comparison of Monte Carlo Methods for Nonlinear Radiation Transport," *Proc. ANS Topical Meeting, International Topical Meeting on Mathematics and Computation* , Salt Lake City, Utah (2001).

[6] R. G. McClarren, "A Robust, High-Order Implicit Monte Carlo Method for Thermal Radiative Transfer," *ANS Winter Meeting and Nuclear Technology Expo*, Vol. 98, p. 501, Washington D.C. (2008), On CD-ROM, American Nuclear Society, LaGrange Park, IL (2008).

[7] A. Wollaber, *Advanced Monte Carlo Methods for Thermal Radiation Transport*, Ph.D. thesis, University of Michigan (2008).

[8] S. Mosher, "Exact Solution of a Nonlinear, Time-Dependent, Infinite-Medium, Grey Radiative Transfer Problem," *ANS Winter Meeting and Nuclear Technology Expo*, Vol. 95, Albuquerque, New Mexico (2006), On CD-ROM, American Nuclear Society, LaGrange Park, IL (2006).

[9] J. A. Fleck, Jr., E. H. Canfield, "A Random Walk Procedure for Improving the Computational Efficiency of the Implicit Monte Carlo Method for Nonlinear Radiation Transport," *J. of Comput. Phys.*, **54**, pp. 508–523 (1984).

[10] J. D. Densmore, T. J. Urbatsch, T. M. Evans, M. W. Buksas, "A Hybrid Transport-Diffusion Method for Monte Carlo Radiative-Transfer Simulations," *J. Comput. Phys.*, **222**, pp. 485–503 (2007).